SSRG International Journal of Mechanical Engineering
ISSN: 2348 – 8360 /doi:10.14445/23488360/IJME-V8I1P101

Volume 8 Issue 1, 1-7, January 2021
©2021 Seventh Sense Research Group®

Prediction Model for DI Diesel Engine: Combustion

Rajesh Kumar Prasad
Department of Mechanical Engineering, Faculty of Science and Technology
ICFAI University Jharkhand, Ranchi-835222, India

Abstract - *Diesel engines are more efficient engines over a century, but the major problem associated with it is the NOx-PM trade-off. Nowadays, controlling this trade-off becomes a challenge due to the limitation of adiabatic flame temperature measurement and the achievement of strict emission norms. This study focuses on developing a simulation tool for predicting combustion phenomena, rate of heat release, and heat transfer from the cylinder without experimentation that consumes labor, time, and cost. A zero-dimensional predictive model is proposed after large numbers of trial & error with selection and coupling of appropriate combustion phenomena. Selected combustion prediction models are further validated for turbocharged diesel engines with experimentation at various loads (50% to 100%) and speeds (1400 rpm and 2200 rpm). It was observed that deviation of peak pressures at 100% load both at 2200 rpm & 1400 rpm are 9% and 3.4%, respectively, but the deviations in at Part loads, i.e., 75% and 50%load are negligible at 2200 rpm while 2.8% and 6% respectively at 1400 rpm.*

Keywords - *Zero-dimensional combustion model, DI diesel engine, Ignition Delay, Rate of Heat Release (ROHR)*

I. INTRODUCTION

Diesel engines have been widely used for automotive either on road, off-road for heavy vehicles, and light-duty vehicles such as trucks, buses, tractors, cranes, cars, etc., due to their superior power to weight ratio[1]. To reduce the research and development cost, low complexity combustion & emissions simulation models need to be implemented into full-cycle diesel engines. The majority of simulation models developed by the various researchers included two-zone emission models [2]. The zero-dimensional single zone combustion model is the simplest one [3, 4], in which fuel-air mixture is considered uniform in composition and temperature at any instant during combustion. Zero dimensional single zone models are used for simulating engine combustion (ignition delay and heat release) and performance with high accuracy [5]. Earlier, this zero-dimensional model is used to predict heat release in which pressure-crank angle data was used as input data [3-6]. Ignition delay Ericson et al. [7] predicted ignition delay using a linear black-box model and gross heat release rate (GHRR). Empirical constants were determined for GHRR based on speed and load on engines. The heat release model developed by Watson et al. [8] is taken care of both premixed and diffusive phases of diesel combustion. Heat loss from the engines is predicted as per Annand correlation [9, 10]. The single-zone model is inferior to estimate the spatial temperature and chemical composition distribution and cannot predict adiabatic flame temperature and emissions [6, 11].

On the other hand, 3D models demand huge computing power, cost, and time and their benefit lower due to empirical correlations [12]. Hence, 0D single-zone and multi-zone models are proposed for simulation of combustion and emissions purposes. However, the majority of earlier published zero-dimensional transient models were used only for combustion [2]. Prediction of "rate of heat release" (RoHR) using Wiebe's function requires a frequent change in statistical function parameters with a change in engine operating parameters [13].

Wilhelmsson et al. [14] developed a NOx prediction model for vehicle on-board and predicted temperature within the two zones (burned and unburned) to avoid iterative energy balance computation. Arsie et al. [15] developed a phenomenological model for the simulation of combustion and NOx-Soot emissions of common-rail multi-jet Diesel engines (swept volume 1.9 liters). The authors used a single-zone model to simulate the ignition delay and combustion during a pilot sequence, pre and main fuel injections for a 1.9-liter engine. The heat release rate was simulated using the Watson model. Andersson et al. [16] also developed a zero-dimensional multi-zone, a fast NOx prediction model for engine optimization, after treatment control or virtual mapping. In this model, cylinder pressure data was used as input data. The Zeldovich mechanism was used to simulate the formation of NO emissions in [14], [15], and [16], respectively. Mellor et al. [17] developed a skeletal mechanism consisting of seven elementary reactions. NOx emissions either in diesel or CNG or hydrogen or HCNG (blends of CNG and hydrogen) are temperature-dependent phenomena, and maximum were occurred at stoichiometric air-fuel ratio and decreases with lean mixtures [18-21]. Those were used to develop a two-zone model for NOx emissions from DI Diesel engines. They reported that Zone-1 was a stoichiometric region (Φ=1) where [NO] formatted by forwarding reactions was small. Zone-2 contains hot burned gases at the overall equivalence ratio. In this zone 2, NO decomposition occurs through the reverse N2O mechanism. Chmela et al. [22] worked on a non-dimensional combustion model based on mixing controlled combustion (MCC Heat Release Rate). This model avoids the detailed description of the individual mixture formation and fuel oxidation processes. It was reported that the rate of heat release (ROHR) is controlled by the instantaneous fuel mass present in the cylinder charge and the local density of turbulent kinetic energy.

II. Experimental Setup & Methodology

4-cylinder 4-stroke turbocharged diesel engine fitted with eddy current dynamometer was selected for the experimental validation of predicted data. Figure 1 shows the experimental engine setup. The detailed specifications of the selected 4-stroke turbocharged direct injection diesel engine were mentioned in table 1.

Table 1: Engine specifications

Engine Type (→) / Engine Specification (↓)	**Turbocharged 4-stroke 4 cylinder DI Diesel**
Bore (mm)/ stroke (mm)	102/ 110
Connecting rod length (mm)	220
IVC (CA)/ EVO (CA)	210/ 540
Rated speed (rpm)	2200
Swept volume (litre)	0.9 per cylinder
Compression ratio	17.4
Injection system	Common rail

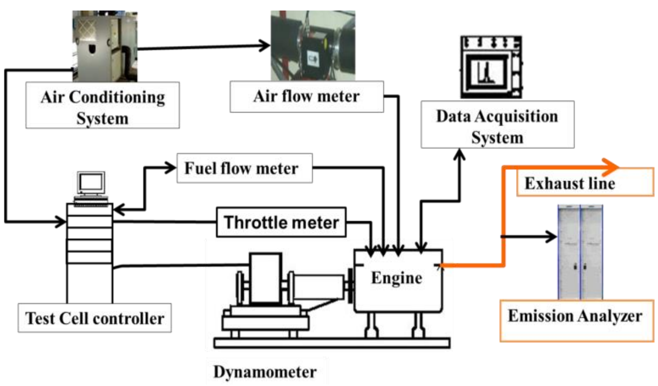

Figure 1: Experimental Engine setup to collect data for validation of simulated results

The parameters noted from the engine experiment were Brake Power (kW), Engine Speed (rpm), Crank angle Measurement, Air Flow Rate (kg/hr), In-cylinder gas pressure measurement (bar), Fuel Flow Rate (kg/ hr), and NOx concentration (g/kWhr).

The model used in this study is zero-dimensional because it does not account for the exact geometric features of the engine combustion chamber. Input data required for simulation are Bore, stroke, connecting rod length, Compression ratio, Inlet and exhaust valve timing, Operating speed, Fuel injected quantity, the start of injection, duration of injection, Inlet manifold pressure and temperature, Air intake depression, and back pressure, Fuel cetane number and lower calorific value. The two-zone combustion model is considered a burned zone responsible for emissions formation and an unburned zone composed of only air and EGR, as explained by Figure 2.

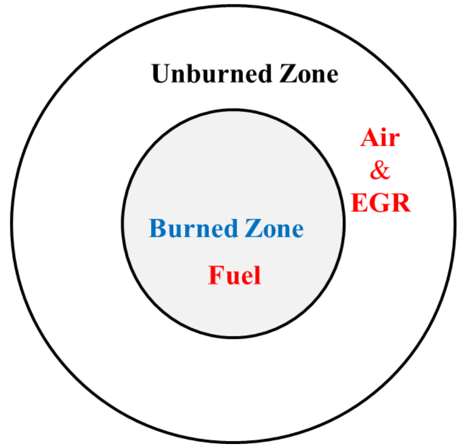

Figure 2: Two-zone concept [5];

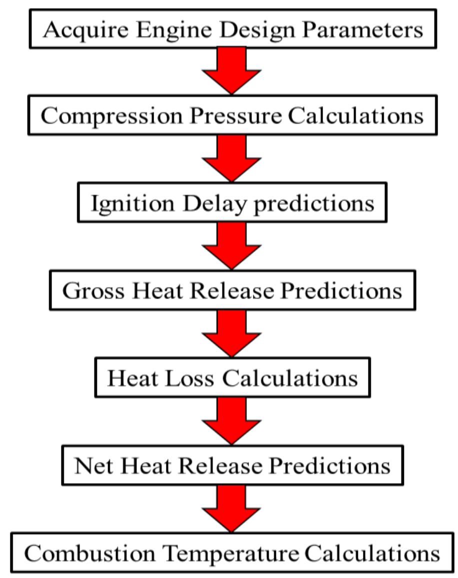

Figure 3: Steps needed to develop a prediction model

Assumptions made to develop the model are listed below:

- Zero dimensional two-zone models.
- The constituents in each zone inside the cylinder behave as an ideal gas.
- Unburned cylinder air is compressed and expanded isentropically.
- Combustion takes place at local stoichiometric conditions.
- There are no pressure gradients inside the cylinder.
- The injected fuel is burned completely.
- Energy released originates from injected fuel only.
- There is no heat transfer among the zones.

Figure 3 shows the steps to be followed for the combustion prediction model. The combustion process in a compression ignition engine is a premixed-diffusion one.

Arrhenius type equations are generally used for ignition delay calculation:

$$\tau_{id} = a\, p^{-n} \exp(\frac{E_a}{R\,T}) \quad (1)$$

Where a, n are constants.

The value of constants chosen in the Arrhenius type equation by Wolfer and Watson are given in table 2:

Table 2: Value of constants for Arrhenius equation

Constants	Wolfer [1]	Watson [5, 23]
a	0.44	3.45
n	1.19	1.02
Ea/ R	4650 K	2100 K

Heywood recommends a correlation for ignition delay, which was developed by Hardenberg and Hase (1979) [24];

$$\tau_{id} = (0.36 + 0.22\, v_p)\, X1.Y1 \quad (2)$$

Where,

$$X1 = \exp[E_a\left(\frac{1}{R_0\,T} - \frac{1}{17190}\right),$$
$$Y1 = \{21.2/(p - 12.4)\}^{0.6}$$
$$E_a = \{1310000/(CN + 25)\}$$

Since the cylinder pressure and temperature are considerably varied during the ignition delay period, the following equation has been developed to account for it [16]:

$$\int_{tsoi}^{tsoc} (\frac{dt}{\tau_{id}}) = 1 \quad (3)$$

The ignition delay time could be evaluated once the above relationship is satisfied:

$$t_{delay} = t_{soc} - t_{soi} \quad (4)$$

Watson model [23] is used for combustion phase modeling. The total combustion process is mainly divided into two major parts; premixed combustion and diffusion combustion. The premixed phase is a consequence of the mixture prepared during the ignition delay period, which burns rapidly, and the diffusion burning phase accounts for the remainder of combustion.

$$m_{fb}(t) = \beta\ f_{pre}(t) + (1-\beta) f_{diff}\ (t) \quad (5)$$

Where,

$$\beta = 1 - \{(a\,\emptyset)/\tau^c\},$$
$$f_{pre(t)} = \{1 - (1 - t^{k_1})\}^{k_2},$$
$$f_{diff(t)} = 1 - \exp(-k_3 \times (t)^{k_4})$$

In equation (5), t is the time measured from the start of ignition, which is non-dimensionalized by the total combustion duration:

$$t = \{t_\theta - t_{ign}\}/\{\Delta t_{comb}\} \quad (6)$$

The best-fit values of k1, k2, k3, & k4 for a range of DI diesel engines, based on a nominal combustion duration of 125^0CA, were found to be

$k_1 = 2.0 + 1.25 \times 10^{-8}\,(\tau_{id}\,N)^{2.4}$; $k_2 = 5000$;
$k_3 = 14.2/\{\emptyset\}^{0.664}$; $k_4 = 0.79 \times \{k_3\}^{0.25}$;
0.8 < a < 0.95; 0.25 < b < 0.45;
0.25 < c < 0.50.

The instantaneous heat transfer across the walls of engines is estimated using Hohenberg's correlation (1979)[24, 25];

$$h_c = \frac{130\, {p_c}^{0.8}\, (v_p + 1.4)^{0.8}}{V^{0.06}\, {T_g}^{0.4}} \quad (7)$$

Convective heat transfer [25]

$$\frac{dQ_{ht}}{d\theta} = h_c A_c (T_{cyl} - T_w)(\frac{1}{6n}) \quad (8)$$

Cylinder pressure or combustion pressure is calculated using the following correlation:

$$\frac{dp}{d\theta} = h_c.A_s\left(\frac{dQ_n}{d\theta} - \frac{\gamma}{\gamma-1} p\,\frac{dV}{d\theta}\right)(\frac{\gamma-1}{V}) \quad (9)$$

The equation for the apparent heat release rate can be determined from the pressure data, is given by;

$$\frac{dQ_n}{dt} = \frac{dQ}{dt} - \frac{dQ_L}{dt} = \frac{\gamma}{\gamma-1}\,p\,\frac{dV}{dt} + \frac{1}{\gamma-1}\,V\,\frac{dp}{dt} \quad (10)$$

The ratio of specific heats (γ) varies with the isentropic compression process or expansion process. The γ is calculated by a relatively simple correlation [25] as follows:

$$\gamma = 1.338 - 6 \times 10^{-5}\,T + 1 \times 10^{-8} T^2 \quad (11)$$

The temperature at every crank angle can be determined by using the Ideal gas equation:

$$p\,V = mR\,T \quad (12)$$

Unburned Zone Temperature [25]

Unburned zone temperature can be calculated using the polytropic relation between temperature and pressure:

$$T_1 = T_0(\frac{P_1}{P_0})^{\frac{\gamma-1}{\gamma}} \quad (13)$$

Burned zone temperature before considering flame temperature can be calculated using the isentropic relationship:

$$T_{exp,1} = T_{burn,0} \times (\frac{P_1}{P_0})^{\frac{\gamma-1}{\gamma}} \quad (14)$$

Burned zone temperature after considering the flame temperature is computed as:

$$T_{burn,1} = \{T_{exp,1} \times m_{burn,0} + T_{flame,1} \times m_{flame,1}\}/\{m_{burn,1}\} \quad (15)$$

III. Results & Discussion

After simulation of zero-dimensional model prediction of engine combustion, it is compared against corresponding experimental data from the multi-cylinder turbocharged diesel engine. Diesel combustion was extensively studied by varying load at a speed of 2200 rpm and a BMEP of 8.6 bar by keeping constant injection timing. Intake manifold temperature was maintained at 105^0 C by providing a cooling system. During the experiments, every measurement was recorded with average data of the 30s at the end of 5 min stabilization of engine for every change of conditions.

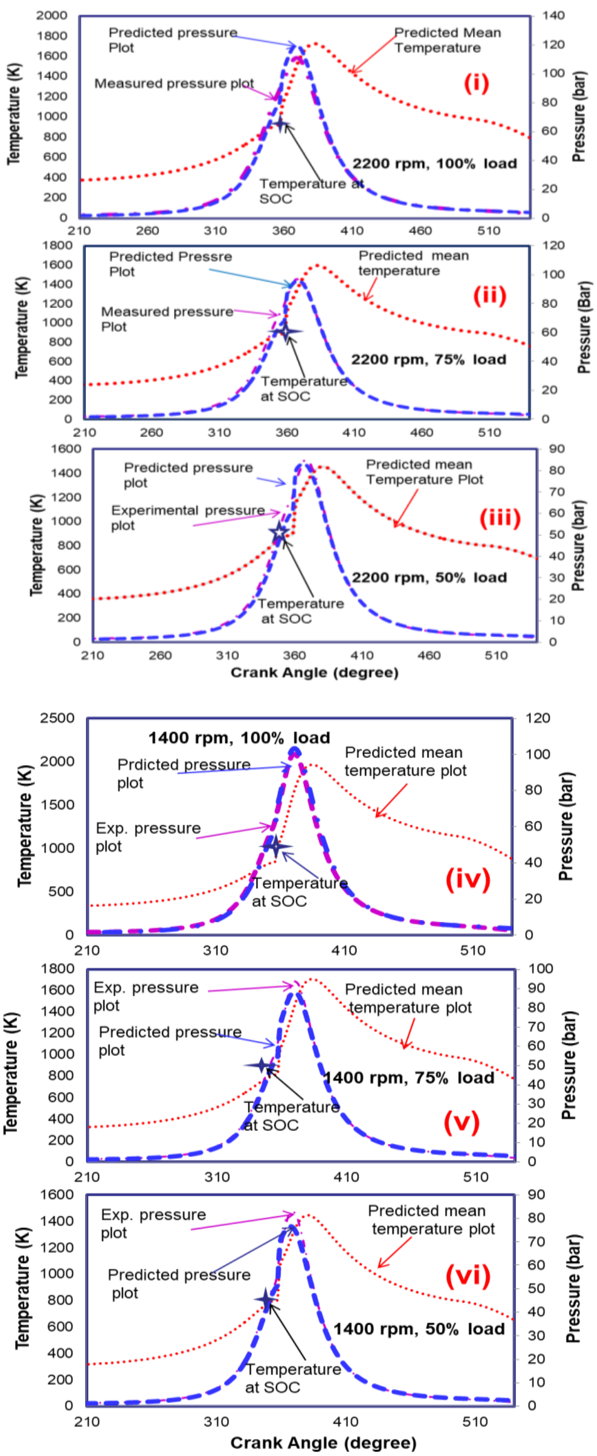

Figure 4: Comparison between Measured Vs. Predicted pressure plot at 2200 rpm and 1400 rpm with varying load

Figure 4 shows the comparison between Measured Vs. Predicted pressure plot at 2200 rpm and 1400 rpm with varying load. In the first, second, and third operating mode (i.e., 2200 rpm and loads of 100%, 75%, 50% respectively), as shown in Figure 4(i), (ii), (iii), both predicted pressure and temperature at the inlet to engine and start of combustion (SOC) are 2 bar, 80 bar, and 378.3 K, 925.6 K respectively. The measured pressure at this mode was 110 bar at 363^0 CA (peak pressure crank angle, $\theta_{p_{max}}$) which is very close to the predicted $\theta_{p_{max}}$ 364.4^0 CA. At this load, the mass of air (387.5 Kg/hr) entrapped into the cylinder resulted in higher pressure and temperature after compression.

It is also observed that due to a decrease in load from 100% to 75%, the pressure reduces from 120 bar to 95 bar but $\theta_{p_{max}}$ Delayed by 2.5^0 CA. This drop-in P_{max} is because of the reduced airflow rate into the cylinder (348.8 Kg/hr compared to earlier mode, 387.5 Kg/hr) and reduced inlet pressure 1.65 bar instead of 2 bar. Comparing the above two modes, the pressure drop is 18, while the drop in temperature is 48.8 K.

In the third operating mode (refer to Figure 4(iii)), engine load reduces from 75% to 50% at 2200 rpm resulted in reduced P_{max} was also reduced from 95 bar to 83 bar. Again if the load on the engine further reduced to 10% at 2200 rpm, then both predicted and measured pressures are identically equal to 65 bar $\theta_{p_{max}}$ They are also identical and equal to 362^0 CA. Inlet pressure was observed to be 1.25 bar, while pressure at SOC was 51.6 bar. Due to lower inlet pressure, we get lower SOC pressure from earlier mode (60.7 bar), but the temperature is nearly identical (888.7 K) because the mass flow rate of air was (269.3 Kg/hr) reduced while inlet temperatures were equal to 358.9K in both cases.

In the fourth, fifth, and sixth case (Figure 4 (iv), (v), (vi)), the engine was operated at 1400 rpm.

If the engine's loadgine reduced from 100% to 75% load at 1400 rpm, then predicted peak pressure was ar educeduces from 103.4 bar to 88.4 bar as shown in figure 4(v). In this condition, the P_{max} measured was 91 bar, and their $\theta_{p_{max}}$ Were 369.5^0 CA and 367^0 CA, respectively. The pressure and temperature at SOC were 54.3 bar and 801.4 K. Air flow rate into the cylinder was 179.4 Kg/hr, lower than the earlier mode (193.1 Kg/hr) the inlet pressure was 1.32 bar instead of 1.43 bar. The drop in pressure & temperature is 3.2 bar & 25.5 K if compared to full load at 1400 rpm.

A further reduction to 50% at 1400 rpm reduces both predicted, and measured pressures were 76.6 bar and 81.5 bar, respectively (refer to figure 4(vi)). It was also observed that $\theta_{p_{max}}$ To 366.5^0 CA and 366^0 CA, respectively. Both inlet and SOC conditions pressures and temperatures reduced to 1.23 bar, 51.2 bar, and 317.2 K, 801.4 K. This reduction is due to low pressure and temperature inlet compared to earlier model.

Effect of load on Heat Release

The heat release rate (HRR) results obtained at various operating modes at 2200 rpm, and 1400 rpm during simulation are compared with experimental validation in figure 7.

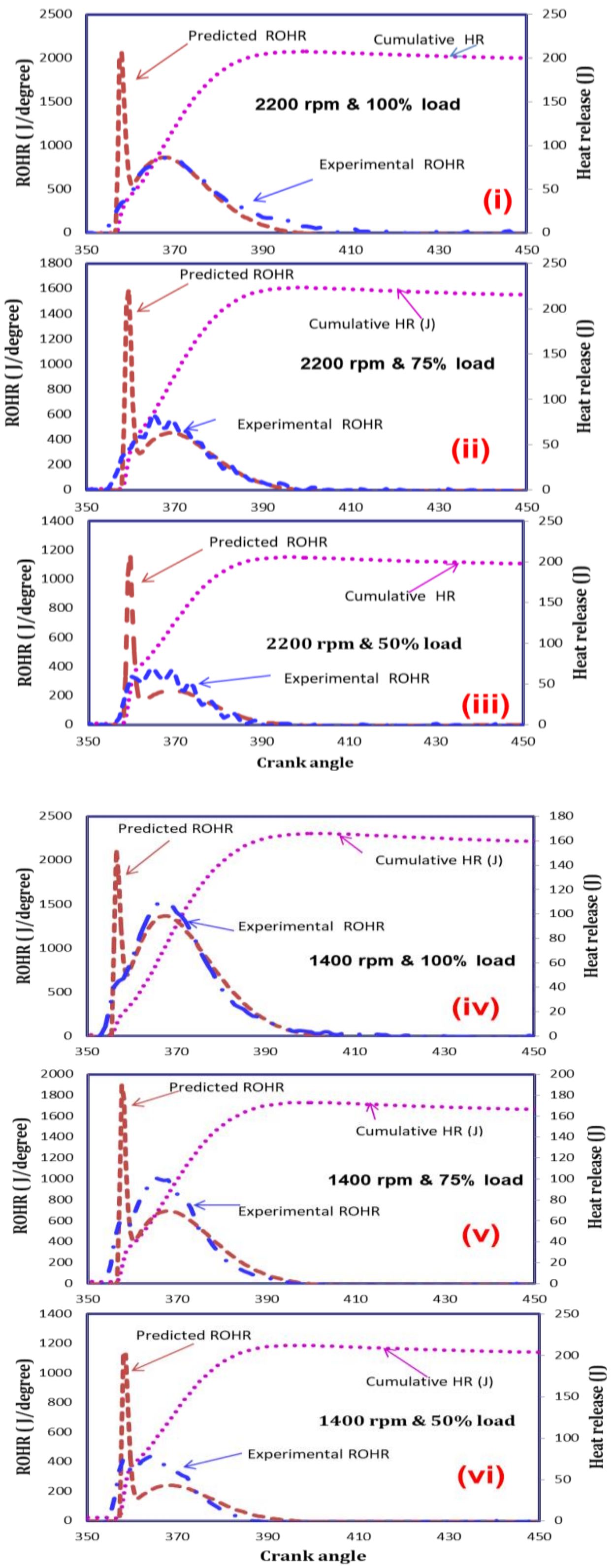

Figure 5: Comparison of predicted and the cumulative rate of heat release (ROHR) at 2200 rpm and 1400 rpm with varying load

The Watson model is used for HRR calculation over Wolfer. To verify the accuracy of different operating modes, experimental data of heat release is compared with the predicted model. In figure 5, the predicted apparent heat release rates are plotted at different operating conditions.

Figure 5(i) shows the comparative results at 2200 rpm with a full load. The mass of fuel injected, equivalence ratio, and actual A/F ratio measured were 50.91 mg per cycle, 0.5099 and 28.83, respectively. The first peak of the HRR is predicted to occur at 3580 CA, while the second occurs at 367.50 CA. The magnitude ROHRmax in premixed combustion is 206 J/degree, while during diffusion combustion, it was reduced to 86.6 J/degree. Experimental data indicate that the diffusion peak occurs at 368 degrees CA and ROHR was 86 J/degree. The presence of higher inlet pressure and temperature at the inlet (2 bar and 378.3 K) resulted from increased pressure and temperature at SOC are 80 bar and 925.6 K, respectively, which increased the fraction of fuel mass burned in the premixed combustion phase by 20.9%. The rest of the fuel mass is burned in the diffusion phase, which starts at 3610 CA.

If the load on the engine was lowered from 100% to 75% (in second operating mode) at 2200 rpm, then the two peaks of ROHRmax are 221.21 J/degree and 63.1 J/degree, and these occurred at 359.50 CA and 3690 CA respectively (refer to figure 5(ii)). In this operating mode, pressure and temperature both at inlet and SOC were reduced to 1.65 bar, 358.9 K, and 62 bar, 876.8 K, respectively, which increased the ignition delay from 5.5 degrees CA to 6.5 degrees CA and also ROHRmax from 206 J/degree to 221.21 J/degree. This increased ROHRmax happen due to increased ignition delay, and thus more % of fuel mass (~ 26.75%) was consumed during the premixed combustion. Diffusion combustion starts delayed to 362.5 degrees CA instead of 361 degrees CA in the first operating mode.

Suppose the engine load was further reduced to 50% at 2200 rpm (in third operating mode). The mass of fuel injected and equivalence ratio reduced to 28.11 mg per cycle and 0.3521, and the actual A/F ratio increased to 41.75 (refer to figure 7(iii)). Reduced pressure and temperature observed both at inlet and SOC are 1.48 bar, 358.9 K and 60.7 bar, 888.6 K, respectively, which increased the ignition delay from 5.5 degrees CA to 7 degrees CA mode and thus increased the ROHRmax from 206 J/degree to 211.63 J/degree. Increased ignition delay results higher % of fuel mass ~37.57% was consumed in the premixed combustion compared to 20.9% at full load (in 1st operating mode). Diffusion combustion starts at 362.5 degrees CA compared to 361 degrees CA at full load.

The engine was operated at full load in the fourth operating mode, but its speed was lowered from 2200 rpm to 1400 rpm. Compared with 1st operating mode (refer to figure 5(i), the recorded data for the mass of fuel injected and equivalence ratio were increased to 56.85 mg per cycle, and 0.727 and actual A/F ratio measured was reduced to 20.21

respectively. The two peaks, ROHRmax, were reduced to 152.77 J/degree and 98.43 J/degree, and these occurred early at 356.5 degrees CA and 367.5 degrees CA, respectively (refer to figure 5 (iv)). The measured ROHRmax during diffusion combustion was 109 J/degree at 367 degrees CA.

In this operating mode, pressure and temperature were reduced both at inlet and SOC are 1.43 bar, 337.7 K and 57.5 bar, 837.7 K, respectively. Reduced temperatures and pressures at 1400 rpm results reduce the ignition delay period from 5.5 degree CA to 5 degree CA and reduce ROHRmax from 206 J/degree to 152.77 J/degree. The % of fuel mass consumed in the premixed phase is ~25.9%. Diffusion combustion starts at 364 degrees CA instead of 361 degrees CA in the first mode.

In the fifth operating mode, engine load was reduced to 75% at 1400 rpm than the two peaks ROHRmax were 189.7 J/degree and 60.6 J/degree, and the corresponding CA in the degree are 357.5 degrees CA and 368 degrees CA respectively (refer figure 7(v)). The measured ROHRmax during diffusion combustion was reduced to 101 J/degree at 365 degrees CA. This operating mode mass of fuel injected, equivalence ratio, and actual A/F ratio measured was 42.44 mg per cycle, 0.5843 and 25.16, respectively.

A similar effect was observed, like 75% at 2200 rpm.

If the engine is further reduced to 50%, similar to the third operating mode but at 1400 rpm (refer to figure 7(vi); sixth operating mode). The magnitude of ROHRmax in premixed combustion was 201 J/degree at 358.5 degrees CA, while during diffusion combustion was 43 J/degree at 368 degrees CA. Experimental data indicate that the diffusion peak occurs at 364 degrees CA and ROHRmax was 78 J/degree. In this operating mode, the mass of fuel injected, equivalence ratio, and actual A/F ratio measured were 28.87 mg per cycle, 0.4211 and 34.91, respectively.

Conclusions

A comprehensive, zero-dimensional two-zone diesel combustion model has been proposed to predict combustion phenomena and adiabatic flame temperature during steady-state operation of a turbocharged diesel engine. Engine loads varied between 50% to 100%, and conditions were simulated in steps at 1400 and 2200 rpm and compared with experimental results. The observations are summarized in the following paragraphs:

- The deviation of peak pressures at 100% load at 2200 rpm & 1400 rpm is 9% and 3.4%, respectively. The deviations in peak pressures at Part loads, i.e., 75% and 50% at 2200 rpm, are negligible but observed to be 2.8% and 6%, respectively, at 1400 rpm.
- Pressure and temperature at the start of combustion mainly depend on inlet condition at the inlet.
- Due to the decrease in load on the engine at particular rpm, the heat release rate decreases, but when the load is constant, and engine speed decreases, the heat release rate increases.
- Due to higher ignition delay at part load, the mass of fuel consumed during the premixed phase is increased. At 2200 rpm speed, 20.9%, 26.7%, and 37.5% of fuel consumed during cycle at 100%, 75%, and 50% load. Similarly at 1400 rpm fuel consumption in premixed phase is 25.9%, 29.8% and 38.2% at 100%, 75%, and 50% load. Therefore, we conclude that due to large fluctuation in load, ignition delay increases.

REFERENCES

[1] Heywood, J.B., Internal Combustion Engine Fundamentals, McGraw Hill Inc., 779(1988) 468-560.

[2] Rakopoulos, C.D., Dimaratos, A.M., Giakoumis, E.G., and Rakopoulos, D.C. Exhaust emissions estimation during transient turbocharged diesel engine operation using a two-zone combustion model. International Journal of Vehicle Design, 49(2009) (1-3)125-149.

[3] Foster, D.E.,An Overview of Zero-Dimensional Thermodynamic Models for I.C. Engine Data Analysis,(1985)SAE 852070.

[4] Assanis, D.N., and Heywood, J.B. “Development and Use of a Computer Simulation of the Turbo compounded Diesel System Engine Performance and Component Heat transfer Studies,(1986) SAE 860329.

[5] Jung, D., and Assanis, D. N.,Multi-zone DI Diesel Spray Combustion Model for Cycle Simulation Studies of Engine Performance and Emissions,(2001), SAE 2001-01-1246.

[6] Guezennec, Y.G., and Wajdi, H.,Two-Zone Heat Release Analysis of Combustion Data and Calibration of Heat Transfer Correlation in an IC Engine., SAE (1999) 1999-01-0218.

[7] Ericson, C., Westerberg, B., Andersson, M. and Egnell, R. “Modelling diesel engine combustion and NOx formation for model-based control and simulation of the engine and exhaust after-treatment systems” (No. 2006-01-0687). 2006, SAE Technical Paper.

[8] Watson, N., Pilley, A.D., Marzouk, M. “A Combustion Correlation for Diesel Engine Simulation,” 1980, SAE 800029.

[9] Rakopoulos, C.D., and Giakoumis, E.G., Diesel Engine Transient Operation, Springer-Verlag London Limited, 2009, pp. 75-76, 319-352.

[10] Annand, W.J. Thermodynamics and Fluid Mechanics Group. Heat transfer in the cylinders of reciprocating internal combustion engines. Proceedings of the Institution of Mechanical Engineers. Jun;177 (1)(1963) 973-96.

[11] Stiesch, G., and Merker, G. P.,A Phenomenological Model for Accurate and Time Efficient Prediction of Heat Release and Exhaust Emissions in Direct Injection, (1999) SAE 1999-01-1535.

[12] Ebrahimi, K., Bazargan, M. and Jazayeri, S.A. A new phenomenological model for combustion and performance studies of direct injection diesel engines (No. 2007-01-1904) (2007), SAE Technical Paper.

[13] Serrano, J.R., Arnau, F.J., Dolz, V. and Piqueras, P. Methodology for characterization and simulation of turbocharged diesel engines combustion during transient operation. Part 1: data acquisition and post-processing. Applied Thermal Engineering, 29(1)(2009) 142-149.

[14] Johansson, B., Wilhelmsson, C., Tunestål, P., Johansson, R. and Widd, A. A Physical Two-Zone NOx Model Intended for Embedded Implementation. 2009, SAE 2009-01-1509

[15] Arsie, I., Di Genova, F., Pianese, C., Sorrentino, M., Rizzo, G., Caraceni, A., Cioffi, P. and Flauti, G.,Development and identification of phenomenological models for combustion and emissions of common-rail multi-jet diesel engines.,(2004), SAE Technical Paper No. 2004-01-1877.

[16] Andersson, M., Johansson, B., Hultqvist, A., and Noehre, C. A real predictive time NOx model for conventional and partially premixed diesel combustion.,SAE Transactions, (2006) 863-872.

[17] Mellor, A.M., Mello, J.P., Duffy, K.P., Easley, W.L. and Faulkner, J.C. Skeletal Mechanism for NO x Chemistry in Diesel Engines., SAE

transactions, (1998) 786-801.

[18] Prasad RK, Mustafi N, Agarwal AK. Effect of spark timing on laser ignition and spark ignition modes in the hydrogen-enriched compressed natural gas-fuelled engine. Fuel. 2020 Sep 15;276:118071.

[19] Prasad RK, Agarwal AK. Experimental evaluation of laser ignited hydrogen-enriched compressed natural gas-fueled supercharged engine. Fuel.;289:119788.

[20] Prasad RK, Agarwal AK. Development and comparative experimental investigations of laser-plasma and spark plasma ignited hydrogen-enriched compressed natural gas-fueled engine. Energy. (2020) 13:119282.

[21] Prasad RK, Agarwal AK. Laser-Ignited Engine Development for Adaptation to Hydrogen-Enriched Compressed Natural Gas (HCNG). InMethanol and the Alternate Fuel Economy 2019 (185-211). Springer, Singapore.

[22] Chmela, F.G. and Orthaber, G.C. Rate of heat release prediction for direct injection diesel engines based on purely mixing controlled combustion., SAE transactions, (1999) 152-160.

[23] Rakopoulos C.D., Giakoumis, E.G., Diesel Engine Transient Operation, Springer,(2009).

[24] Hardenberg, H. O., and F. W. Hase.,An empirical formula for computing the pressure rise delay of a fuel from its cetane number and the relevant parameters of direct-injection diesel engines., SAE Transactions (1979) 1823-1834.

[25] B.P.Pundir. I.C.Engine (Cumbustion and Emissions), Narosa Publishing House Pvt. Ltd., New Delhi, (2007).